

Relationship Between Thermal Properties and Diffusion Coefficients of Gases for Polyimide Films

HIROYUKI TSUZUMI,¹ KEIO TOI,¹ TOMOYASU ITO,² TETSUO KASAI³

¹ Department of Chemistry, Faculty of Science, Tokyo Metropolitan University Minamiosawa, Hachioji, Tokyo 192-03, Japan

² School of Social Information Studies, Otsuma Women's University Kami-oyamada, Tama 206, Japan

³ Mitsubishi Chemical Corporation Research Center, Kamoshida-cho, Midori-ku, Yokohama 227, Japan

Received 20 March 1996; accepted 5 August 1996

ABSTRACT: The relationships between the chemical structure, packing density ($1/V_F$), and cohesive energy density (CED) and the thermal properties of polyimides were investigated. Particularly, the correlation of $\tan \delta$ measured by stress-strain/thermal mechanical analysis with $1/V_F$ and CED was found for eight polyimides. We measured the relationship between the apparent diffusion coefficient (D_a) and $1/V_F$ and CED, respectively, as described in previous articles. From these experiments, we found that the thermal properties, especially $\tan \delta$, were correlated with the apparent diffusion coefficient of gas. These results are well explained by use of micro-Brownian motion. © 1997 John Wiley & Sons, Inc. *J Appl Polym Sci* **64**: 389–397, 1997

Key words: polyimides; SS-TMA; $\tan \delta$; diffusion coefficient; micro-Brownian motion

INTRODUCTION

Many investigators have suggested that the apparent diffusion coefficient D_a of gas is related to the packing density ($1/V_F$) of polyimide,^{1–5} and we additionally have shown that D_a is also related to cohesive energy density (CED).^{6–9} $1/V_F$ was calculated by the reciprocal of specific free volume at 25°C, according to the group contribution method by Bondi.¹⁰ CED was also calculated by the group contribution method of van Krevelen.¹¹ These correlations obtained by us are shown in Figures 1 and 2. Clearly, the diffusivities are highly correlated with the packing density of the polymer, except for two polyimides in Figure 1. These correlations between the diffusion coefficient with the packing density and CED, respectively, are caused by the thermal motions of seg-

ments of polymers, but few investigators have discussed it. In this study, the thermal properties (glass transition temperature, cracking temperature, and $\tan \delta$) of polyimide membranes were measured by differential scanning calorimetry (DSC), thermal gravimeter-differential thermal analysis (TG-DTA), and stress-strain/thermal mechanical analysis (SS-TMA),^{12–13} and the relationship between the thermal properties and the gas diffusivity was discussed.

EXPERIMENTAL

Materials

The structures and characterizations of the polyimides examined in this study are shown in Table I. The polyimides used in this study are based on a dianhydride unit with a diamine unit, which are shown in Table II. The membranes

Correspondence to: K. Toi.

© 1997 John Wiley & Sons, Inc. CCC 0021-8995/97/020389-09

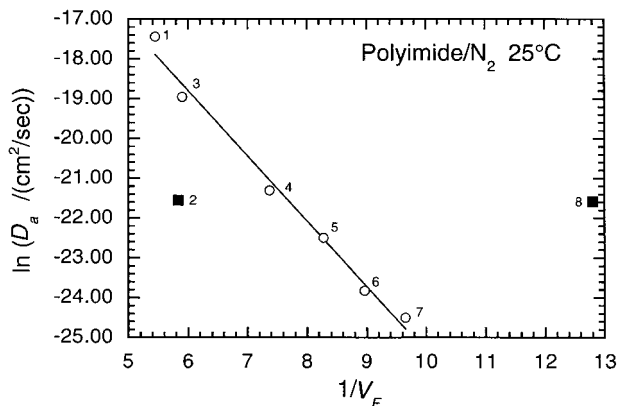


Figure 1 Correlation of the apparent diffusion coefficients for N_2 in polyimides at 25°C with the packing density. The points given by sample number are observed values. The solid line is the linear regression of six points.

used in this study were provided when used in previous studies.⁶⁻⁹

Wide-angle X-ray diffractograms were recorded with an X-ray powder diffractometer CN4037AI (Rigaku Co., Ltd., Tokyo) with Cu-K α radiation ($\lambda = 0.154 \text{ nm}$).^{14,15} The results of the X-ray studies are shown in Figure 3, and the d -spacing of these samples is shown in Table III.

Measuring Apparatuses

A DSC-8240 system, a TG-8101D system, and a TMA-8140 system (called TAS-200) (Rigaku Co., Ltd., Tokyo) were used for this purpose. The TAS-200 system, connected to a microcomputer, PC9801FA (NEC, Tokyo), was used for data col-

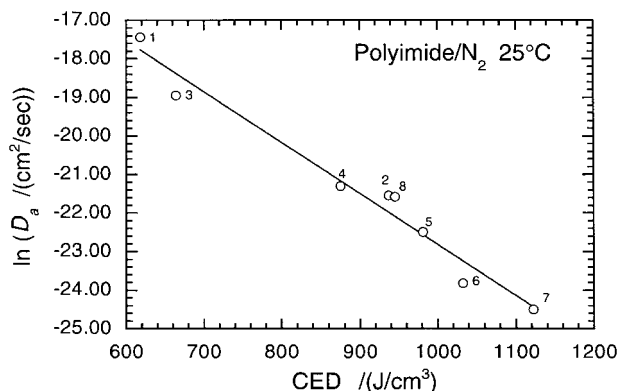


Figure 2 Correlation of the apparent diffusion coefficients for N_2 in polyimides at 25°C with the CED. The points given by sample number are observed values. The solid line is the linear regression of eight points.

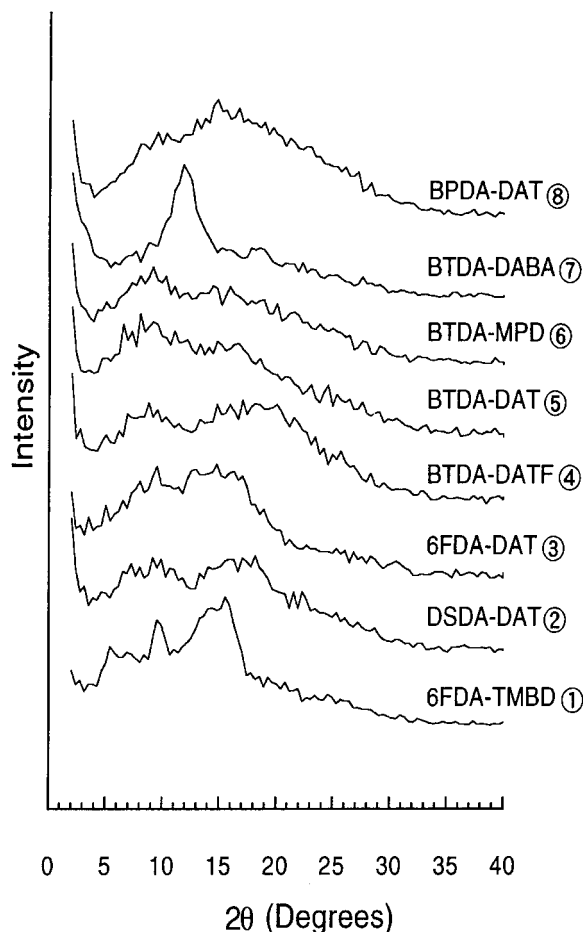


Figure 3 Wide-angle X-ray diffraction scans of the polyimide membranes used in this study.

lection and analysis. All measurements were carried out under a stream of oxygen-free dry nitrogen.

The measurements of the glass transition temperature by the use of DSC are as follows. The samples of finely divided polymer (less than 6 mg in weight) were sealed in an aluminum pan. An empty sample pan was used as a reference. The glass transition temperature with DSC was measured by recordings run at heating rates of $20^\circ\text{C}/\text{min}$. From the glass transition temperature measured by DSC, we predicted the peak of $\tan \delta$ from SS-TMA in the vicinity of this temperature. In addition, by knowing this temperature, we avoided the meltdown of the polyimide membrane in the detector part of SS-TMA.

The cracking temperatures T_1 and T_2 were determined by the use of TG-DTA. The measurements of the cracking temperature by the use of TG-DTA are as follows. The samples of finely divided polymer (4–6 mg) were put in an aluminum

Table I Structures and Characterizations of Polyimides Examined in This Study (Samples Are Aligned So As To Increase $1/V_F$)

		Polyimide							
		1	2	3	4	5	6	7	8
		(6FDA-TMBD)	(DSA-DAT)	(6FDA-DAT)	(BTDA-DATF)	(BTDA-DAT)	(BTDA-MPD)	(BTDA-DABA)	(BPDA-DAT)
Y =									
X =									—
MW (g/mol)		648.56	444.42	530.38	462.34	408.37	394.34	438.35	380.36
d_{25} (g/cm ³)		1.2953	1.3370	1.4266	1.4576	1.3587	1.4031	1.4456	1.4086
$1/V_F$		5.44	5.83	5.90	7.37	8.27	8.96	9.65	12.8
CED (J/cm ³)		618	937	664	875	981	1032	1122	945
$\ln D_a(N_2, 25^\circ\text{C})$		-17.437	-21.545	-18.946	-21.304	-22.491	-23.818	-24.495	-21.579

Substitutions on sites marked Y and X in the following polymer repeat unit:

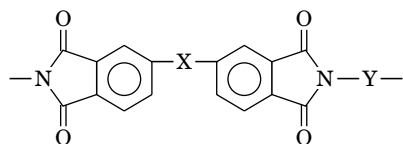


Table II Carboxyl Acid Dianhydrides and Diamines Used for These Measurements

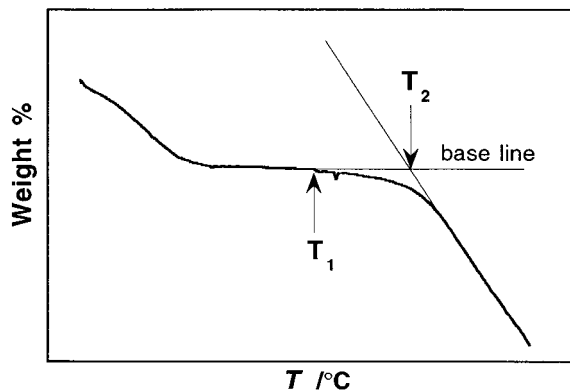
6FDA	3,4,3',4'-diphenyldi(trifluoromethyl)-metanetetra-carboxyl dianhydride
BTDA	benzophenonetetracarboxyl dianhydride
DSDA	3,4,3',4'-diphenylsulfonetetracarboxylic dianhydride
BPDA	3,4,3',4'-biphenyltetracarboxylic dianhydride
TMBD	3,3',3,3'-tetramethylbenzidine
DATF	3,5-diaminotoluene trifluoride
DAT	2,4-diamino toluene
MPD	<i>m</i> -phenylene diamine
DABA	diamino benzoic acid

pan. An empty pan was used as a reference. The cracking temperature with TG-DTA was measured by recordings run at heating rates of 20°C/min. If polyimide is pyrolyzed below the glass transition temperature obtained from the peak of $\tan \delta$ from SS-TMA, then $\tan \delta$ could not be obtained correctly, because polyimide membranes must be pyrolyzed before obtaining $\tan \delta$ at the glass transition temperature. These temperatures are shown in Figure 4. T_1 was determined from the temperature detaching from baseline. T_2 was determined from extrapolation. Usually, T_2 is called the cracking temperature; therefore, T_2 was defined as the cracking temperature in this study. However, T_2 could not be calculated in some polyimide membranes. In this case, T_1 was also calculated.

The measurements of the glass transition temperature and $\tan \delta$ by the use of SS-TMA are as follows. Each polyimide membrane was cut approximately into 10 × 5-mm pieces. We considered that the glass transition temperature is higher than 150°C from the results obtained from DSC. Then, $\tan \delta$ from SS-TMA was measured by

Table III *d*-Spacing Obtained from Wide-Angle X-Ray Diffraction Patterns of Polyimide Membranes Used in this Study

Polyimide	<i>d</i> -Spacing		
6FDA-TMBD 1	13.7	9.3	6.3
DSDA-DAT 2	9.9	5.2	
6FDA-DAT 3	9.2	6.2	5.7
BTDA-DATF 4	9.8	4.8	
BTDA-DAT 5	10.9	9.6	5.7
BTDA-MPD 6	11.5	9.2	5.5
BTDA-DABA 7	11.8	7.4	
BPDA-DAT 8	9.0	5.8	

**Figure 4** Determination method of the glass transition temperature with DSC and the cracking point with TG-DTA.

recordings run at heating rates of 20°C/min below 150°C and run at heating rates of 2.0°C/min above 150°C. The frequency of the load was 0.1 Hz.¹ The value of $\tan \delta$ was kept almost constant below the glass transition temperature, but it changes abruptly and shows a peak when passing the glass transition temperature, as reflected by the micro-Brownian motion of the main chain of polyimides. In this study, the value of $\tan \delta$ is defined by the height of this peak, and the temperature of this peak is defined as the glass transition temperature from SS-TMA.

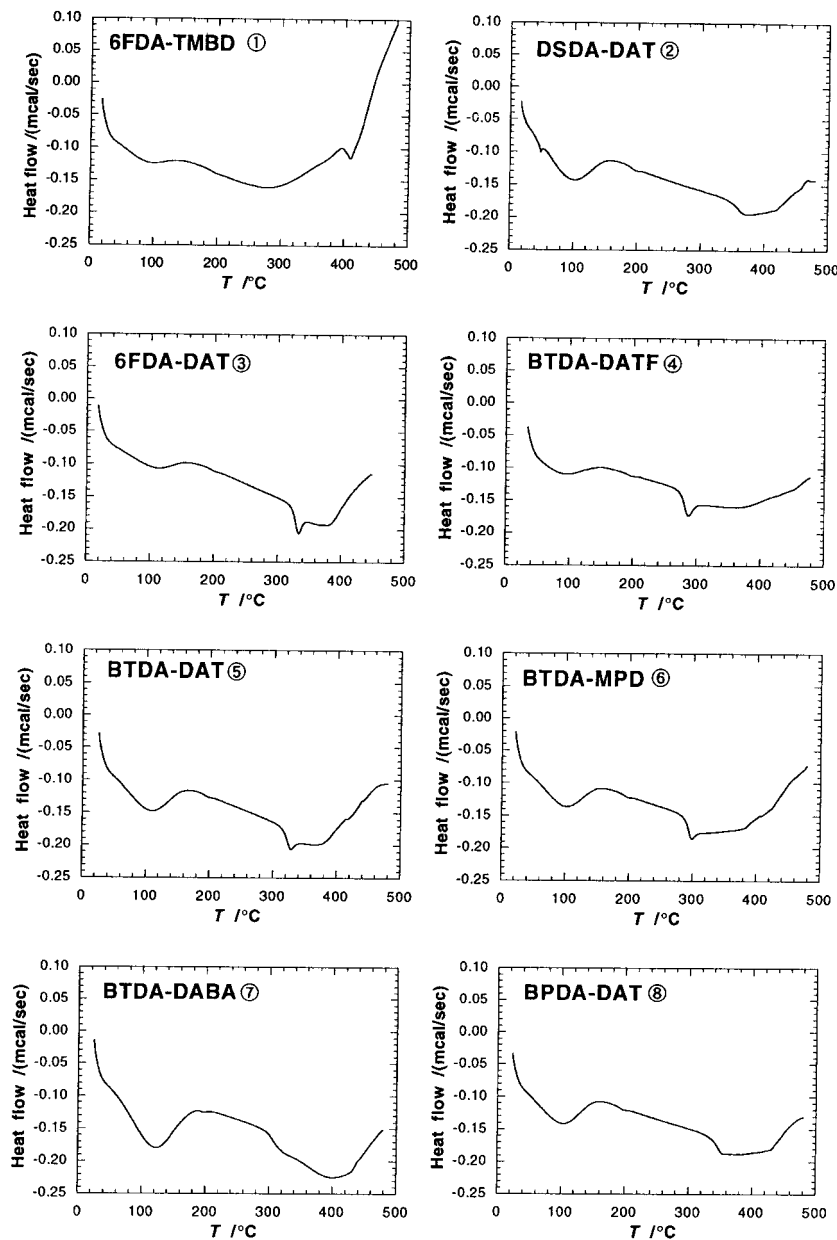
RESULTS AND DISCUSSION

In our previous study,⁶ we showed the correlation of $1/V_F$ and CED with the apparent diffusion coefficient of gases in polyimides, and these correlations are shown in Figures 1 and 2. Clearly, the diffusivities are highly correlated with the packing density of the polymer, except for two polyimides, as shown in Figure 1. The behavior of BPDA-DAT 8 can be rationalized by considering the counteracting effects of packing and torsional mobility of the repeat unit of polyimide on the diffusivity of the penetrant in the polymer. On the other hand, sulfur in the substitute, =SO₂, of DSDA-DAT 2 that combines the two large electronegative oxygens increases electropolarity; then, the mutual interaction of the molecular chains is effective and causes the polymer main chain to pack densely.

The glass transition temperatures obtained from DSC and SS-TMA, the cracking temperature

Table IV Thermal Properties of Polyimide Membranes Used in this Study

Property	6FDA-TMBD 1	DSDA-DAT 2	6FDA-DAT 3	BTDA-DATF 4	BTDA-DAT 5	BTDA-MPD 6	BTDA-DABA 7	BPDA-DAT 8
T_g (°C) (DSC)	397	348	323	276	316	287	298	336
T_g (°C) (TMA)	366	298	245	244	300	210	258	293
Cracking T_1 (°C)	360	308	—	—	336	310	250	265
Cracking T_2 (°C)	400	360	—	—	338	315	338	342
$\tan \delta$ [at T_g (°C)]	—	1.98	4.52	2.36	2.45	2.22	0.688	2.21

**Figure 5** Heat flow curves with temperature for polyimides obtained from DSC.

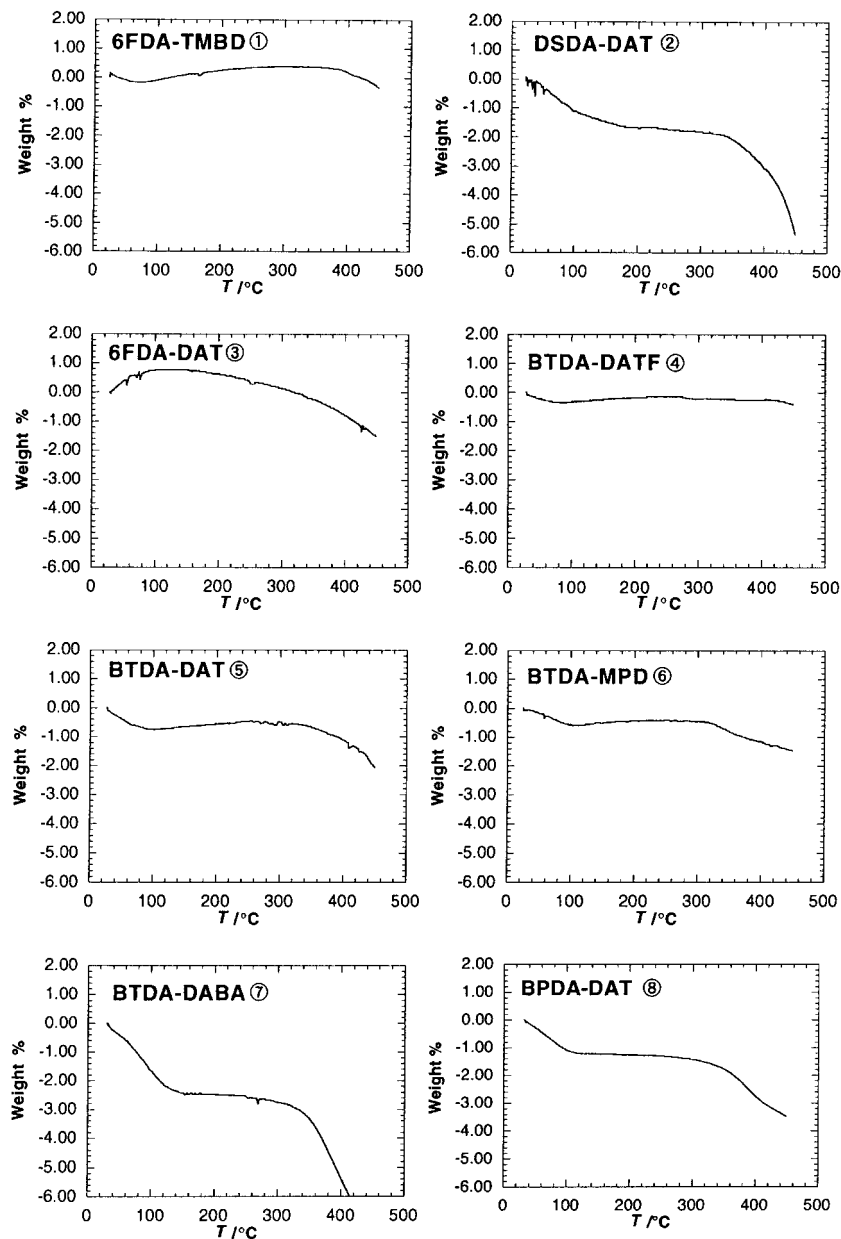


Figure 6 Weight loss curves with temperature for polyimides obtained from TG-DTA.

obtained from TG-DTA, and $\tan \delta$ from SS-TMA are shown in Table IV. The value $\tan \delta$ of 6FDA-TMBD **1** could not be obtained because of the limits of the measurement. The relationships of the heat flow versus the temperature from DSC are shown in Figure 5. The relationships of the percentage of weight loss from TG-DTA versus the temperature are also shown in Figure 6; those of $\tan \delta$ from SS-TMA versus the temperature are shown in Figure 7.²

Some polyimides showed thermal cracking below the glass transition temperature determined

by SS-TMA, as shown in Table IV. However, the weight loss was negligible (less than 0.5%), as shown in Figure 6; then, the thermal cracking was ignored. It is considered that the peak of TG-DTA in the vicinity of 100°C was affected by the adsorbed water in the polyimide, because the polyimides could not be dried completely before these experiments and may contain a trace amount of the adsorbed water.

In general, the glass transition temperature obtained from DSC is higher than the value obtained from SS-TMA. However, the opposite situ-

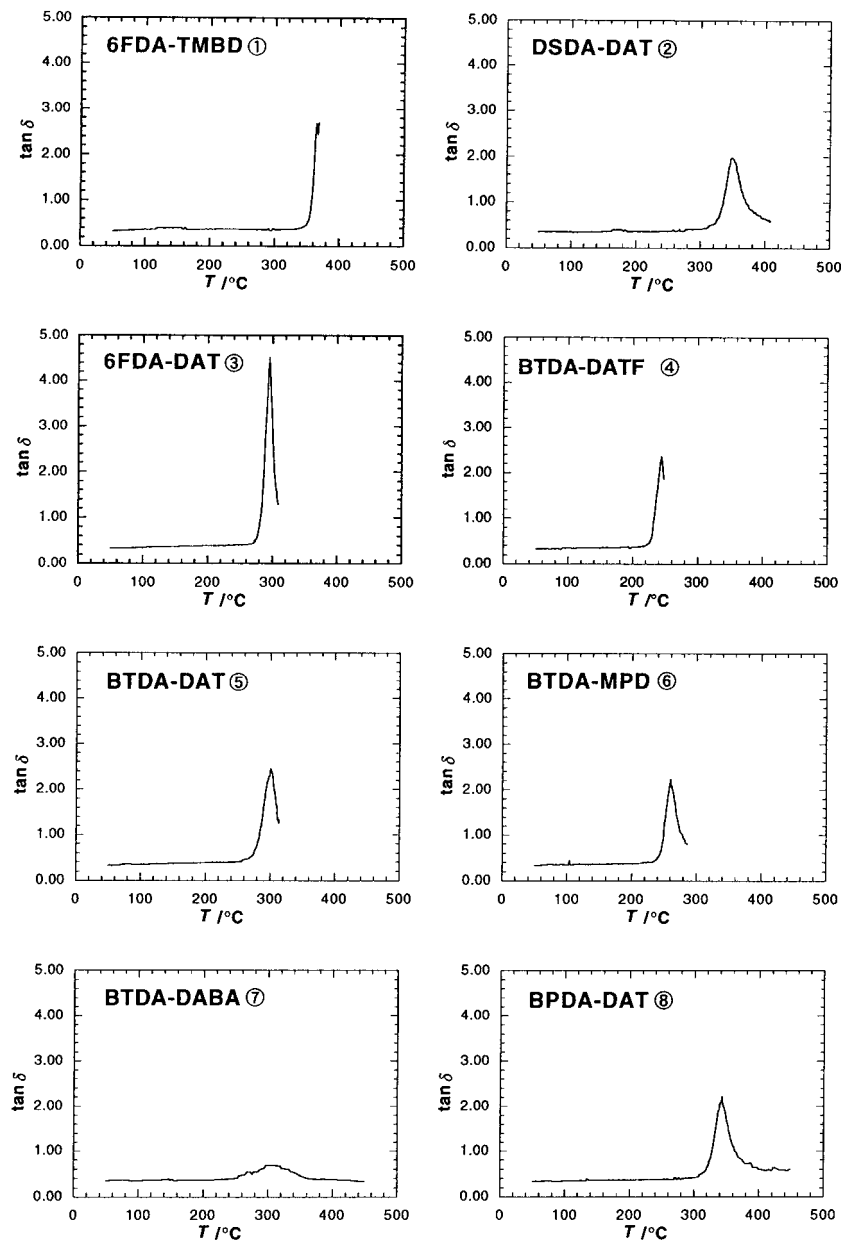


Figure 7 Tan δ spectra for polyimides obtained from SS-TMA.

ation appeared in this experiment.¹³ This is considered as follows. The thermal sensor of DSC detects the temperature of the polyimide membrane directly. On the other hand, the thermal sensor of SS-TMA could not measure the temperature of the membrane directly, but measured the approximate temperature of the polyimide membrane because of the structure of the instrument. In addition, the glass transition temperature obtained from SS-TMA depends on the frequency of the load. Then, the values of glass transition temperature obtained from DSC were distinct

from the values from SS-TMA, but these differences are not important.

The correlation of $1/V_F$ with $\tan \delta$ is shown in Figure 8. At first sight, $1/V_F$ is not related to $\tan \delta$. However, these results exhibit patterns similar to those found in the apparent diffusion coefficients of gas for these polyimides.¹ We tried to remove the two polyimides (DSDA-DAT **2** and BPDA-DAT **8**) that were recognized as an exception in Figure 1; this gives rise to the correlation of $1/V_F$ with $\tan \delta$. When the packing density of the polymer was increased, $\tan \delta$ decreased. As

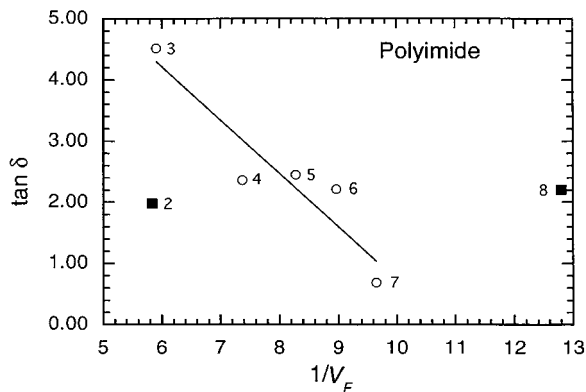


Figure 8 Correlation of $\tan \delta$ at the glass transition temperature with the packing density for polyimides at 25°C. The points given by sample number are observed values. The solid line is the linear regression of five points.

the packing density increased further, however, $\tan \delta$ showed an increase (BPDA-DAT **8**). This behavior can be rationalized by considering the counteracting effects of packing and torsional mobility of the repeat unit of polyimide by the micro-Brownian motion. On the other hand, the substituent of DSDA-DAT **2**, $=\text{SO}_2$, has large electropolarity, causes the polymer main chain to pack densely, and suppress the micro-Brownian motion. Consequently, $\tan \delta$ of DSDA-DAT **2** is rather low. The packing density from Bondi's method for these two polymers cannot be successfully calculated. In brief, the polyimide that has high packing density does not have enough volume for the micro-Brownian motion of the main chain, but the polyimide that has low packing density has enough volume.

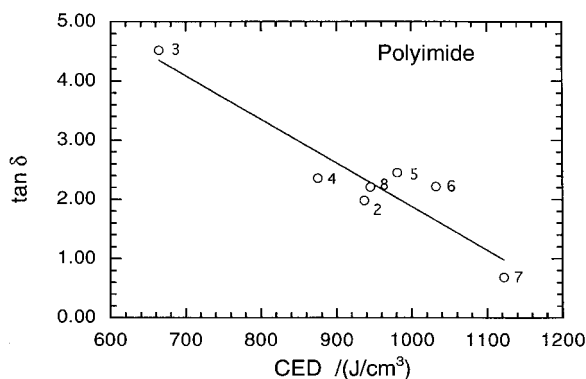


Figure 9 Correlation of $\tan \delta$ at the glass transition temperature with the CED for polyimides at 25°C. The points given by sample number are observed values. The solid line is the linear regression of seven points.

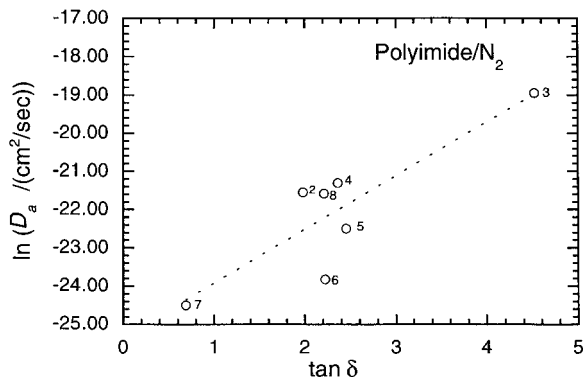


Figure 10 Correlation of the apparent diffusion coefficient for N_2 in polyimides at 25°C with $\tan \delta$ at the glass transition temperature. The points given by sample number are observed values. The dotted line is the linear regression of seven points.

Relationships between $\tan \delta$ and CED are also shown in Figure 9. Without large deviation, a linear regression curve is drawn by calculating seven experimental points. CED is a measure of the cohesive force between molecules, so the polymer chains tend to pack together closely as this value becomes larger. The molecules of the polyimides that have small CED are combined weakly with each other; then, it is considered that the energy barrier of micro-Brownian motion is low and that the micro-Brownian motion of the polymer molecules is active. Therefore, as CED is smaller, $\tan \delta$ is larger.

The correlations of $1/V_F$ and CED with $\tan \delta$ exhibit patterns similar to those found in the diffusion coefficient of gas in polyimides. Then, the correlation of $\tan \delta$ with the apparent diffusion coefficient is easily drawn, as shown in Figure 10. In spite of some scatter, there is a clear tendency for the apparent diffusion coefficient to increase with $\tan \delta$. The apparent diffusion coefficients of N_2 were measured at 25°C, but $\tan \delta$ was measured at the glass transition temperature of each polyimide. In other words, the value of $\tan \delta$ is the peak height measured when the polyimides changed from glassy to rubbery. It is then said that this thermal change influences the gas diffusion into polyimide at 25°C, that is, at glassy state. In addition, two polyimides (DSDA-DAT **2** and BPDA-DAT **8**) that were recognized as an exception in the correlation of the diffusion coefficient with $1/V_F$, as shown in Figure 1, showed the same tendency in the correlation of $\tan \delta$ with $1/V_F$. Then, it can be said that $\tan \delta$ affects the apparent diffusion coefficient directly.

CONCLUSION

The correlations of $\tan \delta$ with $1/V_F$ and CED were found in experiments measured by SS-TMA for eight polyimides. From these experiments, we found that the thermal properties, especially $\tan \delta$, were correlated with the apparent diffusion coefficient of gas. These results are well explained by the use of micro-Brownian motion.

REFERENCES

1. F. R. Sheu and R. T. Chern, *J. Polym. Sci.: Part B: Polym. Phys.*, **27**, 1121 (1989).
2. R. Shimha and G. Carri, *J. Polym. Sci.: Part B: Polym. Phys.*, **32**, 2645 (1994).
3. Y. Maeda, *Homogeneous, Multicomponent Glassy Polymers as Membranes for Gas Separations*, Dissertation, University of Texas, Austin, 1985.
4. S. S. Jordan and W. J. Koros, *Am. Chem. Soc.*, **28**, 2228 (1995).
5. M. Aguilar-Vega and D. R. Paul, *J. Polym. Sci.: Part B: Polym. Phys.*, **31**, 991 (1993).
6. K. Toi, H. Suzuki, I. Ikemoto, T. Ito, and T. Kasai, *J. Polym. Sci. Part B: Polym. Phys.*, **33**, 777 (1995).
7. K. Toi, K. Saito, Y. Suganuma, T. Ito, and I. Ikemoto, *J. Appl. Polym. Sci.*, **46**, 1939 (1992).
8. K. Toi, T. Ito, I. Ikemoto, and T. Kasai, *J. Polym. Sci.: Part B: Polym. Phys.*, **30**, 497 (1992).
9. K. Toi, T. Ito, T. Shirakawa, H. Ichimura, and I. Ikemoto, *J. Appl. Polym. Sci.*, **29**, 2413 (1984).
10. A. Bondi, *Physical Properties of Molecular Crystals, Liquids, and Glasses*, Wiley, New York, 1968.
11. D. W. van Krevelen, *Properties of Polymers*, Elsevier, Amsterdam, 1976.
12. C. G. Bazuin and A. Eisenberg, *J. Polym. Sci.: Part B: Polym. Phys.*, **24**, 1137 (1986).
13. I. Abranitoyannis, I. Kolokuris, J. M. V. Blanshand, and C. Robinson, *J. Appl. Polym. Sci.*, **48**, 987 (1993).
14. Y. Obata, K. Okuyama, S. Kurihara, Y. Kitano, and T. Jinya, *Am. Chem. Soc.*, **28**, 1547 (1995).
15. M. R. Pixton and D. R. Paul, *J. Polym. Sci.: Part B: Polym. Phys.*, **33**, 1353 (1995).